- Technical Paper -

PREDICTED METHOD FOR BOND STRESS BEHAVIOR DEPENDED ON CRACK WIDTH IN CORRODED REINFORCED CONCRETE

Wei DONG[*1], Hideki OSHITA[*2], Shuichi SUZUKI[*3] and Tomoaki Tsutsumi[*4]

ABSTRACT

It is very difficult to accurately estimate the bond stress of cracked reinforced concrete due to the corrosion of rebar, as there are many factors that affect the bond stress, including corrosion ratio of rebar, speed of electrolysis test, tensile concrete stress, rust transfer, and so on. In this paper, corroded specimens with cracks in the concrete cover were tested, and the method for estimating bond stress is suggested. The data shows that it is feasible to estimate the bond stress based on three major factors: corrosion ratio of rebar, corrosion crack width and tensile concrete stress.

Keywords: bond stress, tensile concrete stress, plastic stage, internal pressure

1. INTRODUCTION

Reinforced concrete can encompass many types of structures and components. At use stage, cracks occur in concrete, and corrosion results in the formation of rust of which volume has two to four times of the original volume. Rust reduces strength capacity as a result of both the reduced cross-sectional area and corrosion cracks in the surface rebar. It is well known that the bond stress degrades dramatically, as rebar embedded in concrete are corroded. To illustrate the mechanism of bond stress is very important, and it is a precondition to estimate the residual load capacity of reinforced concrete. For these reasons, recent researchers on predicted models have taken a high toll, and many results have been obtained. However, there is still no accurate estimated model.

Based on this background, the objective of this study is to propose a model to estimate bond stress of corroded reinforced concrete.

2. BOND ACTION OF NON-CORRODED RC

In the previous literature [1], a concrete ring model was used to analyze the bond stress at an elastic stage, a plastic stage, and an elastic stage with internal ring crack. The non-corroded confirmatory experiments in that paper illustrate that many of the data are in the region between a plastic stage and an elastic stage with internal ring crack. Moreover, it shows the tendency that the stress state is much closer to plastic stage.

The stress distribution at plastic stage can be shown in Fig. 1. The plastic stage represents the highest possible bond resistance for the model at the instant that crack occurs in the longitudinal cover. Hence, the maximum internal pressure can be expressed as Eq. 1.

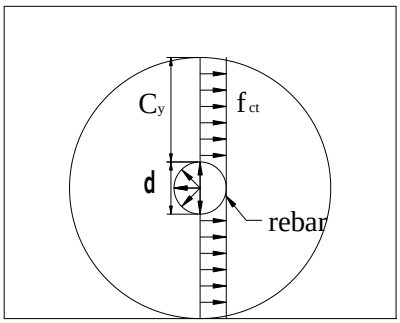

Fig.1 Stress distribution at plastic stage

$$p_i = \frac{f_{ct} \cdot 2c_y}{d} \quad (1)$$

where,

p_i : maximum internal pressure (N/mm^2)

f_{ct} : ultimate tensile concrete stress (N/mm^2)

c_y : thickness of cylinder (mm)

d : internal diameter (mm)

The interaction force makes an angle β with the axis of rebar due to the presence of ribs. The interaction force can be resolved into radial (internal stress) and tangential (bond stress) component (see Fig.2). Eq. 2 can be obtained.

$$p_i = \tau \cdot \tan\beta \quad (2)$$

where,

β : angle between the surface of rib and the rebar axis

τ : maximum bond stress (N/mm^2)

*1 PhD Student, Graduate School of Faculty of Science and engineering, Chuo University, JCI Member
*2 Professor, Graduate School of Faculty of Science and engineering, Chuo University, JCI Member
*3 Tokyo Electric Power Services co., LTD, JCI Member
*4 Doctor, Institute for Technology Development, Tokyo Electric Power co., LTD, JCI Member

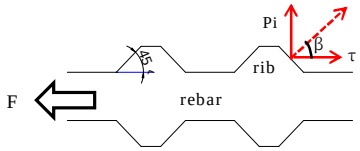

Fig.2 Component of interaction force

3. BOND ACTION OF CORRODED RC

In this study, a predicted method for bond stress of cracked RC beams is promoted in both elastic stage and plastic stage.

3.1 Bond action in the cracked elastic stage

Because the thicknesses of concrete surrounding rebar vary in arbitrary direction, the stress state of rectangular RC specimen is different from that of thick walled cylindrical model. Fig. 3(a) shows the dimension of FEA model both before and after corrosion crack. The dimension is 120mm*100mm, and the concrete cover is 40mm. Internal pressure of 2.5N/mm^2 is applied on internal surface. Positive value denotes tensile stress and negative denotes compressive stress. Before cracking (see Fig.3(b)), the tangential stress at bottom is larger; hence the corrosion crack will occur at concrete cover. After cracking, the distribution of stress is more complicated, for the discontinuity of concrete cover.

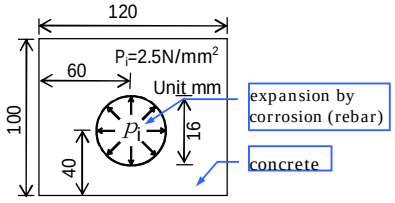

(a) Dimension of FEA model

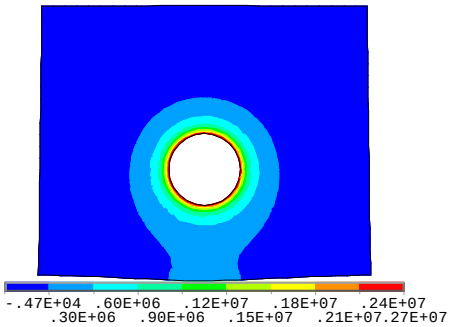

(b) Tangential stress distribution before corosion (unit N/m^2)

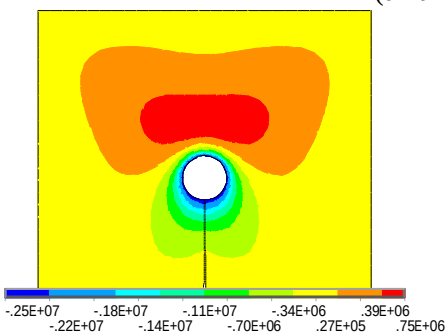

(c) Radial stress distribution after cracking (unit N/m^2)

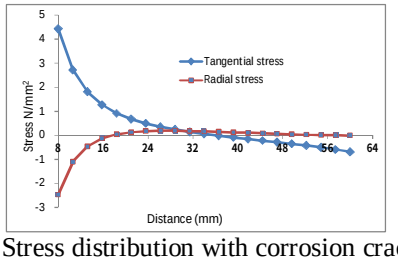

(d) Stress distribution with corrosion crack

Fig.3 FEA solution at elastic stage

Fig.3(c) indicates that the radial compressive stress near crack is extremely larger than upper region, and tensile stress act in the horizontal direction. On this occasion, if the vertical component of internal force exceeds the tensile capacity of concrete cover, failure crack extends along horizontal corrosion crack.

The distribution of radial and tangential stress in horizontal concrete cover is shown in Fig. 3(d). Tangential stress is larger than radical stress, Hence splitting failure easily occur, duo to the formation of crack in horizontal concrete cover. The mechanical model can be shown in Fig.4.

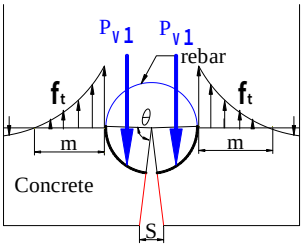

Fig.4 Mechanical mode in elastic stage

If the concrete performs in a perfectly elastic stage, the horizontal crack occurs when the maximum tangential stress in the horizontal direction exceeds the ultimate tensile stress of the concrete. Assume the vertical line passing the center of rebar is the axis of symmetry of corrosion crack, and θ is the angle between horizontal axis of rebar and corrosion crack can be calculated as follows:

$$\theta = \pi/2 - S/2c \tag{3}$$

where,

S : width of crack which is changing with internal pressure (mm)

c : concrete cover depth in crack direction (mm)

The vertical force acting on concrete with unit length can be calculated as follows:

$$P_V = 2P_{vi} = 2\int_0^{\theta} \sin\theta \cdot p_i \cdot \frac{d}{2} d\theta \tag{4}$$

where,

d : diameter of rebar (mm)

p_i : internar pressure (N/mm^2)

The tensile force acting on concrete with unit length can be calculated as follows:

$$F = 2\int_m f_t(m) \cdot dm \tag{5}$$

where,

$f_t(m)$: tensile stress at point on line m (N/mm^2)

m : region of integration of tensile stress (mm)

Although the shape of the distribution of tangential stress is similar to that of thick walled cylindrical mode, the peak stress of cracked model is much higher, compared at the condition with same internal pressure. Based on the balance of force and Eq. 2, bond stress can be calculated as follows:

$$\tau = \frac{2\int_m f_t(m)\cdot dm}{d(1-\sin(S/2c))\tan\beta} \qquad (6)$$

3.2 Bond action in the cracked plastic stage

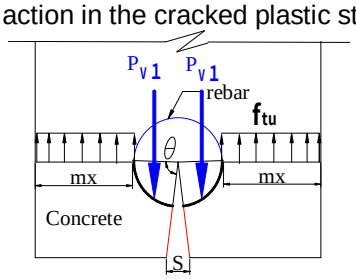

Fig.5 Mechanical mode in plastic stage

In plastic stage, crack will not occur in concrete untill every point at the plane of horizontal concrete cover has reached the ultimate tensile concrete stress. At this moment, the bond stress between concrete and rebar can be expressed as

$$\tau = \frac{2 f_{tu}\cdot m_x}{d(1-\sin(S/2c))\tan\beta} \qquad (7)$$

where,

f_{tu} : ultimate tensile stress of concrete (N/mm^2)

m_x : length of concrete cover in horizontal direction (mm)

4. EXPERIMENT

4.1 Specimens and Parameter

In order to investigate the predicted method, the previous experiment of reinforced concrete beam and pullout test are cited. The meanings of alphabet in the name of specimens are shown in Fig. 6. The schematic of specimens are shown in Fig. 7, and the dimensions are list in Table 1. The characteristics of rebar are shown in Table 2, and the mix proportion, with design compressive strength of 30MPa, is given in Table 3. Moreover, in order to prevent strain gauges from corrosion, they are set inside one tensile rebar, with spacing of 48mm. In order to identify the rebar, two outside tensile rebar are named L and R, and middle rebar, if any, is named M. (See Fig. 7). The concrete covers of all the specimens are all 40mm.

4.2 Method of corrosion

In this experiment, in order to short the time spent on corrosion, and control the corrosion process easily, the method of electrolysis test is adopted [2]. Tensile reinforcements are anodes electrode, copper mesh is a cathode electrode and 18.9A current flows across the two electrodes, till the electric charge in coulombs transferred meets the demands. The specimens are deposited in 5% NaCl solution.

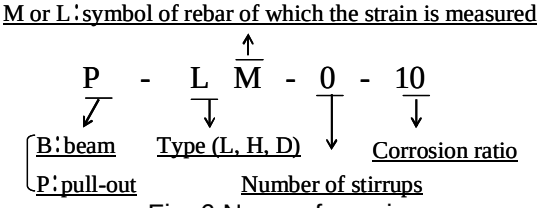

Fig. 6 Name of specimens

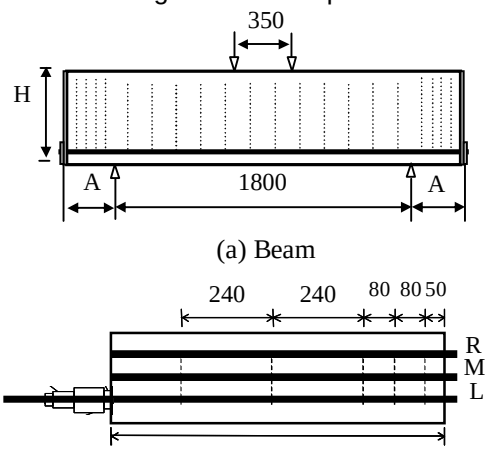

Fig. 7 Schematic of specimens

Table 1 Dimensions of specimens Unit [mm]

Series	height	Width	Length	Length of anchorage
B-L	200	240	2100	150
B-H	260	210		
B-D	340	240	2400	300
P-L	200		875	
P-H	260	210		

Table 2 characteristics of rebar

	Nominal Area (mm^2)	Yield stress (N/mm^2)	Tensile strength (N/mm^2)	Elastic modulus
D22	387.1	400	579	2.0×10^5
D16	198.6	369	523	
D6	31.7	438	557	

Table 3 Mix proportion of concrete

Gmax (mm)	W/C (%)	SL (cm)	Air (%)	Unit weight (kg/m^3) W	C	S	G	Admixture	NaCl
20	60	10	5	168	280	826	996	2.8	8.8

4.3 Test and Measurement

All the beam specimens are monotonically tested untill failure with four-point flexural loading. The loading span and supported span are 350mm and

1800mm respectively. They were loaded under displacement control at a velocity of 0.5mm/min. In the specimens of pullout test, tensile force applied on rebar increased at the speed of 9.8kN/min.

The measured items included load, the axial strain of tensile rebar, corrosion ratio, and so on.

4.4 Corrosion pattern

The corrosion crack propagation is determined by the corrosion ratio, concrete strength, and the losing rust during the electrolysis test. The width of corrosion crack at concrete cover can be measured directly. Take corrosion crack of one pullout specimen for example, shown in Fig. 8(a). It is easy for corrosion crack occur along two outside rebar, however, it is difficult to appear along middle rebar. Fig. 8(b). shows the corrosion ratio of rebar. It is evident the rebar were uniformly corroded.

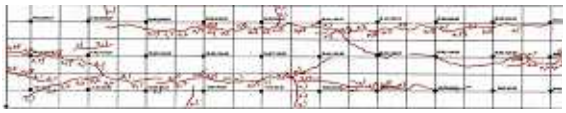

(a) Corrosion crack in concrete cover B-LM-0-20

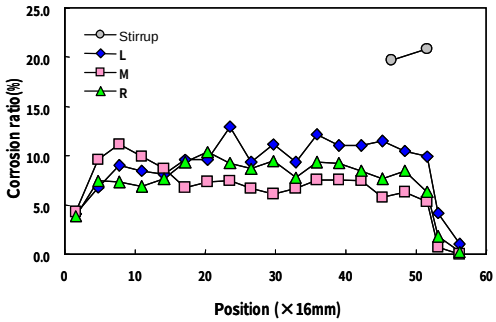

(b) Corrosion ratio P-LM-2-10

Fig. 8 Corrosion pattern

4.5 Data analysis

Each of the specimens has two or three main rebar. However, the effect of internal pressure of each rebar was ignored. Based on the corrosion cracks of these beam, not only the corrosion crack at bottom surface, but also the corrosion cracks in horizontal direction are taken into account. The corrosion crack model and mechanical mode are shown in Fig.9. With regard to the corrosion cracks in the concrete cover, the width at failure stage should be used based on the estimated model. As there is no such data, the width of corrosion cracks is used in the next calculation. In this section, parameters affect the bond stress will be discussed.

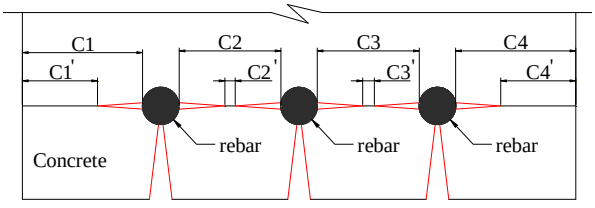

(a) Model of corrosion crack propagation

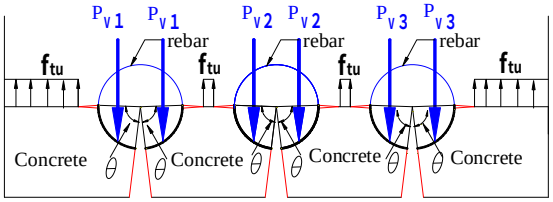

(b) Mechanical model

Fig. 9 Corrosion crack and mechanical model

(1) Region for calculation

The beams performed bond failure was adopt, as the bond stress in anchorage reached the maximum. With regard to pullout specimen, the region is from one gauge, at which rebar has yielded or the strain reached maximum, to another gauge, of which the strain is zero.

(2) Ultimate tensile stress at bond splitting failure

Both the effect of concrete and the stirrups is taken into account. The part of concrete is evaluated with ultimate tensile stress of concrete by splitting tension test. With regard to the part of stirrups, both the residual mass ratio and number of stirrups are taken into account, it can be expressed as follows:

$$f_{st}/f_t = \gamma \cdot n \tag{8}$$

where,

f_{st} : increcement of tensile strength owing to stirrups due to confined effect (N/mm^2)

f_t : tensile strength of concrete (N/mm^2)

γ : residual mass ratio of stirrups

n : number of stirrups in unit calculated region

Hence the proposed equation for estimated tensile strength of specimen f_{tu} can be expressed as below.

$$f_{tu} = f_t + f_{st} = f_t \cdot (1 + \gamma \cdot n) \tag{9}$$

(3) Effective width of concrete

With corrosion, the corrosion cracks propagate at horizontal direction. Therefore, the effective width of concrete becomes shortened. Here define effective width of concrete to denote the width of concrete where cracks have not occurred. Moreover the concrete located between two rebar is affected by individual two rebar, and the corrosion crack is longer. For simplify, coefficient 0.5 is multiplied. Eq. 10 Shows the calculation of specimens with three rebar.

$$\begin{cases} C_1' = (1-\lambda)\cdot C_1 \\ C_2' = \dfrac{1}{2}(1-\lambda)\cdot C_2 \\ C_3' = \dfrac{1}{2}(1-\lambda)\cdot C_3 \\ C_4' = (1-\lambda)\cdot C_4 \end{cases} \tag{10}$$

where,

λ : coefficient of crack propagation

C_1, C_2, C_3, C_4: width of concrete before corrosion (mm)

C_1', C_2', C_3' C_4': effective width of concrete

(*mm*)

(4) Function of λ

Function of λ is important to estimate bond strength. However, it is hard to measure the horizontal crack along the rebar, but it can be seen on the ends of the beam. For simplicity, it is assumed that the coefficient of crack propagation λ only depend on the local corrosion ratio of rebar. It is evident that λ is 1, when the horizontal crack approaches to the side surface of the specimens; and that λ is 0, when the rebar is not corroded. In this study, when the corrosion ratio of side rebars reach to 25%, the horizontal crack reaches to the side surface. That is to say, the coefficient λ is 1, when corrosion ratio α is 25. Moreover, the crack on the end of the beam shows that coefficient λ is approximately equal to power function. Therefore Eq.11 is adopted.

$$\lambda = 2.4(\alpha/100)^{2/3} \tag{11}$$

where,

α : corrosion ratio of rebar (%)

(5) Tensile force of concrete

As the width of crack was not measured during load test, only bond stress in plastic stage is calculated in this paper. The tensile force of concrete per unit length at failure stage can be expressed as Eq 12.

$$F_t = f_t \cdot \sum_{i=1}^{4} C_i' \tag{12}$$

(6) Vertical force acting on concrete by rebar

The vertical force applied on the surface of bottom concrete by rebar can be expressed as Eq 13.

$$P_V = 2\sum_{i=1}^{3}\int_0^{\theta_i} \sin\theta_i \cdot p_i \cdot \frac{d_i'}{2} d\theta = \sum_{i=1}^{3} d_i' p_i (1-\sin(s_i/2c)) \tag{13}$$

Table 4 Test data

Specimen	maximum experimental bond stress	Total tensile strength f_t	Total C'i	corrosion ratio of rebar (%)			width of crack in concrete cover (mm)			diameter			$\sum_{i=1}^{4}\int_0^{\theta_i}\cos\theta \cdot d'd\theta$	p_i inner pressure	estimated bond force τ
	N/mm^2	N/mm^2	mm	L	M	R	L	M	R	L	M	R	mm	N/mm^2	N/mm^2
B-LM-0-10	1.6	2.3	70.4	10.7	8.0	12.0	0.6		0.9	15.9	15.9	15.9	44.5	1.8	1.8
B-LM-0-20	0.7	2.3	36.4	17.7	12.4	15.1	2.4		2.4	15.9	15.9	15.9	41.8	1.0	1.0
B-HL-0-10	3.2	2.1	73.2	13.1		7.1	0.4		0.2	15.9		15.9	29.8	2.6	2.6
B-HL-0-20A	1.2	1.7	15.0	22.6		22.5	0.3		0.1	15.9		15.9	27.8	0.5	0.5
B-HL-0-20B	2.5	2.5	32.6	23.4		13.4	0.5		0.5	15.9		15.9	28.3	1.4	1.4
B-HL-2-20	2.4	1.9	63.1	8.6		10.7	0.3		0.2	15.9		15.9	30.0	2.0	2.0
B-HL-3-20	2.0	1.8	78.3	13.3		5.6	0.4		0.3	15.9		15.9	29.9	2.3	2.3
B-HL-4-20	2.5	2.0	77.1	4.4		4.7	0.5		0.9	15.9		15.9	30.4	2.5	2.5
B-DM-150-10	3.2	2.4	109.7	2.9	0.0	3.9	0.1	0.1	0.1	22.2	22.2	22.2	65.7	2.0	2.0
B-DM-300-10	1.6	2.3	88.0	5.3	3.2	8.3	0.1	0.1	0.0	22.2	22.2	22.2	64.6	1.6	1.6
B-DM-4-10	2.4	2.1	89.6	3.1	7.9	4.5	0.2	0.0	0.0	22.2	22.2	22.2	64.7	1.5	1.5
B-DM-4-5	2.2	2.2	95.0	4.9	4.5	3.8	0.2	0.0	0.0	22.2	22.2	22.2	65.0	1.6	1.6
P-LL-0-0	3.0	2.0	149.4	0.0	0.0	0.0	0.0	0.0	0.0	15.3	15.3	15.3	45.9	3.3	3.3
P-LM-0-0	3.1	2.1	135.6	0.0	0.0	0.0	0.0	0.0	0.0	16.0	16.0	16.0	48.0	3.0	3.0
P-LL-0-10	2.0	2.5	71.1	10.3	7.5	8.7	0.1	0.0	0.1	15.3	15.1	15.0	43.4	2.1	2.1
P-LM-0-10	2.5	1.9	57.8	9.8	16.6	8.7	0.1	0.0	0.1	14.6	14.4	15.0	41.3	1.3	1.3
P-LL-0-20	1.7	1.9	52.8	17.9	9.9	10.7	0.2	0.0	0.1	14.9	15.0	14.9	41.6	1.2	1.2
P-LM-0-20	3.4	1.9	110.0	2.3	2.2	2.0	0.2	0.1	0.1	15.6	15.5	15.6	45.9	2.3	2.3
P-LL-80-0	3.5	2.0	135.6	0.0	0.0	0.0	0.0	0.0	0.0	16.0	15.7	15.7	47.5	2.9	2.9
P-LM-80-0	3.7	2.8	135.6	0.0	0.0	0.0	0.0	0.0	0.0	15.7	15.9	15.7	47.4	4.1	4.1
P-LL-80-10	2.2	2.4	75.9	10.9	5.8	6.9	0.1	0.1	0.0	15.3	15.3	15.2	43.9	2.1	2.1
P-LM-80-10	2.5	2.6	72.6	10.4	8.4	6.8	0.1	0.1	0.1	14.9	15.4	15.2	43.4	2.2	2.2
P-LL-80-20	1.8	2.5	68.0	6.9	7.4	14.1	0.1	0.0	0.2	15.0	15.2	14.6	42.4	2.0	2.0
P-LM-80-20	1.6	2.4	26.9	18.1	18.4	21.4	0.2	0.0	0.1	14.3	15.3	14.0	38.9	0.8	0.8
P-LL-2-10	1.7	2.4	71.5	10.8	8.8	6.5	0.2	0.2	0.1	15.0	15.0	15.2	43.0	2.0	2.0
P-LM-2-10	1.5	2.1	71.2	10.3	7.6	8.6	0.3	0.0	0.2	14.9	15.1	15.1	42.9	1.8	1.8
P-LL-2-20	1.6	2.4	44.7	20.9	13.0	10.3	0.3	0.0	0.1	14.3	14.7	14.9	40.3	1.3	1.3
P-LM-2-20	1.6	2.1	52.0	10.8	19.2	9.0	0.1	0.2	0.1	14.9	14.5	15.0	41.2	1.4	1.4
P-LL-4-10	2.6	2.2	73.7	12.8	6.9	5.2	0.2	0.0	0.2	15.2	15.2	15.3	43.6	1.8	1.8
P-LM-4-10	3.8	2.4	81.8	5.0	10.5	4.7	0.2	0.1	0.2	15.3	14.8	15.4	43.8	2.3	2.3
P-LL-4-20	2.0	2.2	42.7	20.9	14.2	10.7	0.2	0.0	0.2	14.7	14.6	14.9	40.4	1.1	1.1
P-LL-240-0	3.8	2.2	135.6	0.0	0.0	0.0	0.0	0.0	0.0	15.5	15.7	15.7	47.0	3.2	3.2
P-LM-240-0	3.2	2.2	135.6	0.0	0.0	0.0	0.0	0.0	0.0	15.7	15.8	15.7	47.3	3.2	3.2
P-LL-240-20	3.0	2.2	48.3	18.5	11.2	12.0	0.2	0.1	0.2	14.4	14.8	14.8	40.6	1.3	1.3
P-LM-240-20	1.4	2.2	37.7	12.9	22.6	13.9	0.1	0.2	0.1	14.7	14.2	14.6	39.6	1.0	1.0
P-HL-0-0	4.8	2.2	116.7	0.0		0.0	0.0		0.0	15.7		15.7	31.4	4.1	4.1
P-HL-0-10	2.0	2.0	71.7	6.3		6.6	0.1		0.2	15.3		15.2	29.3	2.4	2.4
P-HL-0-20	1.1	1.7	47.4	12.7		11.9	0.4		0.1	14.6		14.8	27.3	1.4	1.4
P-HL-2-10	2.3	2.0	72.9	7.2		5.2	0.2		0.2	15.8		15.3	30.0	2.4	2.4
P-HL-2-20	1.1	2.0	61.1	10.4		7.3	0.5		0.1	14.5		15.2	28.0	2.2	2.2
P-HL-3-20	1.3	2.2	44.1	15.4		11.0	0.5		0.1	14.6		14.9	27.2	1.7	1.7
P-HL-4-20	1.1	2.2	42.1	14.8		12.7	0.5		0.2	14.9		14.7	27.2	1.7	1.7
P-HL-110-0	3.3	1.9	116.7	0.0		0.0	0.0		0.0	15.4		15.7	31.1	3.6	3.6
P-HL-110-10	2.4	1.9	63.1	10.9		5.8	0.5		0.1	14.5		15.3	28.2	2.1	2.1
P-HL-110-20	2.9	1.9	29.3	18.4		16.5	0.7		0.2	14.3		14.4	26.0	1.1	1.1

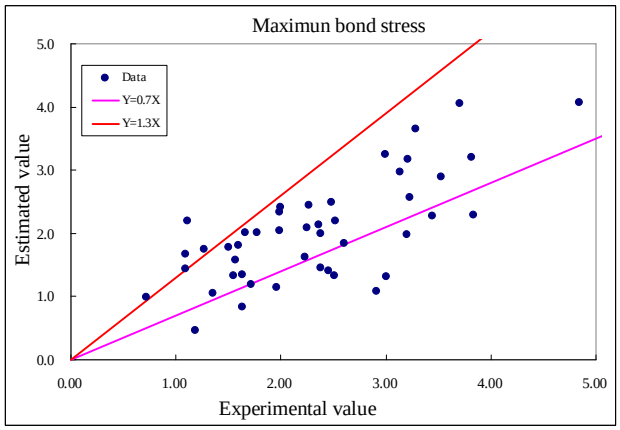

Fig. 10 Relation between experimental and estimated value

where,

d' :diameter of rebar after corrosion (mm)

p_i : internar pressure (N/mm^2)

S_i : width of corrosion crack

c : concrete cover in crack direction (mm)

θ_i : the angle between horizontal axis of rebar i and corrosion crack

i :number of rebar

Assuming that the bond stresses of rebar are the same, the Eq. 14 can be obtained.

$$P_V = p\sum_{i=1}^{3} d_i' \{1-\sin(s/2c)\} \tag{14}$$

(7) Angle β

In reality, the angle between rib and the axis of rebar is changing during corrosion. However the relation between the angle of rib and corrosion ratio is not clear. Hence, it is better to use the constant value of 45° [5], and neglecting the changing of angle.

$$\beta = 45° \tag{15}$$

(8) Bond stress

Based on equilibrium at failure stage, $F_t = P_V$, and equation $p_i = \tau \cdot \tan\beta$, the estimated equation of bond stress can be established as Eq. 16.

$$\tau = \frac{f_t \cdot \sum_{i=1}^{4} C_i'}{\sum_{i=1}^{3} d_i'(1-\sin(s/2c))\tan\beta} \tag{16}$$

(9) Experimental mean bond stress

The experimental value of local bond stress is calculated by Eq. 17.

$$\tau_{loc} = -\frac{1}{\pi\sqrt{1-\alpha_{loc}}\cdot d}\frac{dP_s}{dx} \tag{17}$$

Where,

τ_{loc} : local bond stress (N/mm^2)

p_s : axial force of tensile rebar (N/mm^2)

α_{loc} : local corrosion ratio of rebar (%)

d : diameter of tensile rebar (mm)

x : position of strain gauge (mm)

In calculating the axial force of rebar, the degradation of yield strength due to corrosion was taken into account, and the local yield strength was calculated by Eq. 18.[3]

$$f_{sc} = f_{so} - 2.43\cdot\alpha_{loc} \tag{18}$$

where,

f_{sc} : yield strength after corrosion (N/mm^2)

f_{so} : nominal yield strength (N/mm^2)

α_{loc} : local corrosion ratio of rebar (%)

4.6 Estimated bond stress

The estimated bond stress is calculated based on model. However, the next terms must be clarified.

4.7 Comparison

The value of both experimental and estimated maximum bond value is list in Table 4. The relation between experimental and estimated value is shown in Fig. 10, which indicates that the many of the data is in $\pm 30\%$ region. It is reasonable to simplify the mechanical model as shown in Fig. 5, and it is feasible to estimate the maximum mean bond stress by promoted method in this paper.

5. CONCLUSIONS

(1) The internal bond stress of cracked reinforced concrete can be estimated by corrosion ratio of rebar, corrosion crack and tensile strength of concrete.

(2) The maximum bond stress of cracked reinforced concrete can be estimated by internal stress.

REFERENCES

[1] Tepfers, R.,"Cracking of Concrete Cover along Anchored Deformed Reinforcing Bars," Magazine of Concrete Research, Vol. 31, No. 106 pp.3-11, Mar. 1979

[2] Yuki Murakami, Tetsuhide Kinoshita, Shuichi Suzuki, Yukinari Fukumoto, Hideki Oshita. "Study on the residual strength for corroded reinforcement beam." Concrete Journal, 17(1), pp.61-74, 2006

[3] Yuki Murakami, Hideki Oshita, Shuichi Suzuki, Tomoaki TSUTSUMI. "Study on influence of shear reinforcement and anchorage of residual strength of RC beams with reinforcement corrosion." JSCE, vol.64 No. 4, pp.631-649, 2008

[4] Japan Society of Civil Engineers "Standard Specifications for Concrete Structures for Structural Performance Verification.", 2002

[5] Japanese Industrial Standards "JIS Handbook for Concrete.", 2003